Scientific paper

Fluorination of Mixed γ-alumina/γ-gallia Xerogels with Trifluoromethane: Some Effects on Bulk and Surface Characteristics

Andrii Vakulka,[1,3] Janez Kovač,[2] Gašper Tavčar[1] and Tomaž Skapin[1,3,*]

[1] *Department of Inorganic Chemistry and Technology, Jožef Stefan Institute, Jamova 39, SI-1000 Ljubljana, Slovenia*

[2] *Department of Surface Engineering and Optoelectronics, Jožef Stefan Institute, Jamova 39, SI-1000 Ljubljana, Slovenia*

[3] *Jožef Stefan International Postgraduate School, Jamova 39, SI-1000 Ljubljana, Slovenia*

** Corresponding author: E-mail: tomaz.skapin@ijs.si; Tel.: +386-1-477 3557; Fax: +386-1-477 3155*

Received: 03-07-2012

Dedicated to Prof. Dr. Boris Žemva, recipient of the 2011 Zois Award for the lifetime achievements in inorganic fluorine chemistry.

Abstract

Interaction of single γ-Al_2O_3 and γ-Ga_2O_3, and mixed γ-Al_2O_3/γ-Ga_2O_3 xerogels with CHF_3 at intermediate temperatures results in partial fluorination. Fluorinated oxides remain amorphous and retain a considerable part of the initial surface area; for the fluorinated Al-based materials surface areas in all cases exceed 100 $m^2\ g^{-1}$. Lewis acidity of mixed oxides, either before or after fluorination, is strongly influenced by the presence of surface Ga^{3+} ions, mainly due to their strong preference to replace highly acidic Al^{3+} ions in tetrahedral positions. Ion replacement leads to the formation of acidic sites with lower strengths what is confirmed by the model catalytic reaction, isomerisation of CCl_2FCClF_2. XPS investigations indicate that fluorination of mixed oxides is accompanied by substantial surface reconstructions and preferential formation of Al–F based phases with Ga remaining mainly in O environments. Further segregation processes, such as slow crystallisation of $Al(F,OH)_3{\cdot}nH_2O$ phases, are probably promoted by water adsorption.

Keywords: Alumina, gallia, solid solution, fluorination, triflurometh ane, acidity

1. Introduction

In contrast to alumina (Al_2O_3), which is one of the most intensively studied oxides, research of gallia (Ga_2O_3) received much less attention. Due to some distinctive structural and other similarities between the two families of oxides, Ga_2O_3 polymorphs are frequently studied in comparison with the respective Al_2O_3 analogues.[1,2] Although Ga_2O_3-based or Ga-containing materials are known catalysts for some applications, see for example related references in,[2] it appears that current interest is oriented mainly towards mixed Al_2O_3/Ga_2O_3 catalysts. Good catalytic performance of these materials was observed in selective catalytic reduction (SCR) of nitrogen oxides by hydrocarbons,[3–6] in dehydration of alkanes,[7] and in cracking reactions.[8] As noted in several reports, improved catalytic behaviour of mixed oxides was, besides other factors, associated with higher Lewis acidity that originates from unique arrangements of Ga^{3+} ions found only on surfaces of mixed Al_2O_3/Ga_2O_3.[4,7,8]

Fluorination of Al_2O_3 is a well known procedure to modify, *i.e.* mainly increase, its Lewis acidity and to achieve catalytic activity in reactions that require acid sites of relatively high strength.[9] For these purposes, high surface area γ-Al_2O_3 precursors are usually treated with various fluorinating agents. Among the latter, HF,[10–12] SF_4[13,14], NH_4F,[15] and different hydrofluorocarbons, like $CHClF_2$[16,17] or CHF_3[10–12,17–19], were most frequently used. Besides surface modification, fluorination also induces some structural and morphological changes.[10,11] Extent of these changes strongly depends on the level of fluorina-

tion. For highly fluorinated γ-Al_2O_3, bulk conversion to fluoride is observed with the formation of crystalline AlF_3 phases. Commercial γ-Al_2O_3 fluorinated with CHF_3 at 623 K was for example used as a partially fluorinated benchmark to compare catalytic activity of diverse AlF_3-based materials.[10,19] On the other side, systematic studies of the fluorination of Ga_2O_3-based materials were apparently not undertaken to a greater extent. In an earlier study, fluoride doped Al_2O_3/Ga_2O_3 catalysts were prepared and the promoting effect of the added fluoride was demonstrated in some cracking and hydrocracking reactions.[20] Mixed Al_2O_3/Ga_2O_3 catalysts were also found to be highly active in hydrolytic decomposition of the very stable CF_4. Catalytic activity was correlated with the amount of Lewis acid sites that was increasing with the increasing Ga_2O_3 content up to the optimal value of 20 mol.%. It was also found that addition of Ga_2O_3 stabilised the surface area during the hydrolytic reactions.[21,22]

In the present study a series of mixed γ-Al_2O_3/γ-Ga_2O_3 xerogels was fluorinated at intermediate temperatures. Some work on both single components, γ-Al_2O_3 and γ-Ga_2O_3, is also included for comparison. All fluorinations were performed with trifluoromethane, CHF_3, that proved to be a safe alternative fluorinating agent with the fluorinating capability comparable to HF.[10,11,18] Main intention of the work is to identify and determine the key changes in surface and bulk characteristics that originate from the partial conversion of oxide precursors to fluorides. These aspects are important in further development of related materials with tailored characteristics for possible catalytic applications.

2. Experimental

Preparation of oxide xerogels: Single γ-Al_2O_3 and γ-Ga_2O_3, and mixed γ-Al_2O_3/γ-Ga_2O_3 xerogels were prepared from inorganic precursors following the procedures from previous reports.[23,24] Commercial aluminium nitrate, $Al(NO_3)_3{\cdot}9H_2O$, (Merck, p. a., min. 98.5%) was used; aqueous solution of gallium nitrate, $Ga(NO_3)_3$, was prepared by dissolving metallic gallium (Alfa Aesar, 99.9%) in nitric acid (AppliChem, p. a., 65%). For the preparation of mixed xerogels, aqueous solutions of both nitrates were premixed in proportions corresponding to the Al/Ga ratios given in Table 1. Gelatinous hydroxide hydrogels were prepared from 0.5 molar solutions of single or mixed nitrate(s) by the addition of aqueous ammonia solution (AppliChem, p. a., 25%) under vigorous stirring. Final pH was adjusted to 6–7. Due to the reported difficulties in the preparation of γ-Ga_2O_3 from systems containing excessive water[1,25], all hydrogels were filtered and thoroughly washed with distilled water, and immediately transferred into a preheated muffle furnace where they were dried at 723 K for 24 h.

Throughout the text, single Al_2O_3 and Ga_2O_3 xerogels are denoted as Al#0 and Ga#0, respectively. Mixed Al_2O_3/Ga_2O_3 xerogels are denoted as Al/Ga-x where x represents the nominal Al/Ga atomic ratio, e.g. sample with the nominal molar ratio of Al_2O_3:Ga_2O_3 = 100:1 is denoted as Al/Ga-100. Compositions of mixed xerogels prepared within this study are given in Table 1.

Fluorination: Oxide xerogels were fluorinated with trifluoromethane, CHF_3, (Matheson Europe, min. 98%) under dynamic conditions in a plug flow reactor made of nickel tube with 5 mm ID. Layer of the solid reactant was supported by a plug made of pressed silver wool. Same flow reactor set-up was used also for catalytic tests and pyridine adsorption (see below). Two sets of fluorination runs were performed: (i) for the preparation of larger batches of fluorinated materials for further investigations and (ii) temperature programmed fluorination (TPF) aimed to compare reactivities of different oxides towards CHF_3. In a typical preparative fluorination, oxide xerogel, 1–1.2 g, was fluorinated under a steady flow of CHF_3, 20 vol.% in N_2, for 2 h at constant temperatures specified in Table 1. Fluorinated products are marked with the extension -F. TPF experiments were performed with approximately 100 mg of oxide that were pre-treated in situ at 673 K in flow of N_2. After cooling to room temperature, a constant flow of CHF_3, 33 vol.% in N_2, was applied and the temperature of the reactor was raised linearly to 673 K with a heating rate of 1.8 K min^{-1}. In both sets of fluorination runs, progress of fluorination was monitored by on-line FTIR spectroscopy, as described below.

Chemical analysis: Total fluoride content in fluorinated solid products was determined by direct potentiometry using fluoride ion selective electrode after decomposition of solid samples in $NaKCO_3$ melts.[26]

FTIR spectroscopy: Infrared spectra were recorded on Spectrum GX FTIR spectrometer (PerkinElmer). Spectra of the solid samples, usually recorded with 2 cm^{-1} resolution, were obtained with a MTEC Model 300 photoacoustic detector. Spectra obtained in this way are denoted as PA-FTIR spectra. During the transfer to the photoacoustic cell, samples were for a short time in contact with ambient air. On-line IR-monitoring of gaseous effluents from various tests in the flow reactor was performed with a 10 cm gas flow cell equipped with NaCl windows. During the runs, spectra of the gaseous effluents were recorded continuously with predetermined scanning rates; usual rate was 5 scans min^{-1}. Afterwards, component-specific evolution profiles were constructed from the batch data using the capabilities of the Spectrum TimeBase (PerkinElmer) software. As demonstrated recently, carbon monoxide, CO, is a suitable marker for following reactions between CHF_3 and various oxygen-containing solids since it allows a clear and unhindered distinction from other components in the IR-spectra of bulk gaseous effluents.[27] Same approach was used also in the present study; CO evolution profiles were constructed from the line at 2120 cm^{-1}. In some temperature programmed experiments, pro-

files for H_2O were constructed from the line at 3845 cm^{-1} and those for HF from the line at 4075 cm^{-1}.

Powder X-ray diffraction (XRD): Powder diffractograms of oxide precursors and fluorinated products were recorded on AXS D4 Endeavor diffractometer (Bruker) using Cu $K_{\acute{a}}$ radiation. Before analysis, each sample was slightly grinded to obtain a sufficiently uniform and compact layer on the sample holder.

Catalytic tests: Catalytic behaviour of some representative fluorinated oxide xerogels in isomerisation of 1,1,2-trichlorotrifluoroethane, CCl_2FCClF_2, and subsequent dismutations was investigated under steady flow conditions. Catalytic line and basic test conditions were similar to those used in previous comparative investigations using various AlF_3-based materials as catalysts.[10,13,19] Each catalytic test consisted of two consecutive stages: firstly the temperature was steeply increased to 623 K (activation stage), active materials were afterwards tested at steeply reduced temperatures, down to 523 K. Analyses of the gaseous effluents were performed by on-line gas chromatography after 1 h stabilisation period at each temperature ramp.

X-ray photoelectron spectroscopy (XPS): XPS analyses were carried out on the PHI-TFA XPS spectrometer exciting a sample surface by X-ray radiation from Al monochromatic source. The samples were in the form of 1 mm thick pressed pellets. The analysed area was 0.4 mm in diameter and the analysed depth was 2–5 nm. The XPS survey and narrow scan spectra of emitted photoelectrons were taken with pass energies of 187 eV and 29 eV, respectively. With pass energy of 29 eV energy resolution of 0.6 eV was obtained on the Ag $3d_{5/2}$ peak. During analysis, XPS spectra were shifted due to sample charging; neutraliser gun for low energy electrons was used to reduce this effect. The binding energy 284.8 eV for C 1s peak was used as reference energy for spectra alignment. The spectra of Al 2p, Ga 2p, Ga 3d, O 1s, C 1s and F 1s were acquired during XPS analyses. Relative sensitivity factors provided by instrument producer were used to calculate surface concentrations.[28] The composition was calculated in the model of homogenous matrix. We estimate that the relative error for calculated concentrations is about 20 % of reported values. Error in binding energy was 0.3 eV.

Pyridine adsorption: Pyridine adsorption followed by photoacoustic spectroscopy of chemisorbed pyridine (PAS-py) were performed according to the procedure reported earlier.[16,29] Before pyridine adsorption, samples were conditioned in a flow of N_2 at 523 K for 1 h. Afterwards, reactor was cooled to 423 K and 3 µl of liquid pyridine were injected directly into the reactor inlet where they were immediately evaporated. After pyridine injection, reactor was flushed with N_2 for additional 15 min to remove excessive and physically adsorbed pyridine from the system.

In another set of experiments, thermal stability of pyridine adsorbed on oxides and fluorinated products was investigated by preadsorbing pyridine at room temperature followed by linear heating of the pyridine-loaded materials under flow of N_2 to 673 K (oxides) or 623 K (fluori-

Table 1. Denomination and properties of single and mixed oxide precursors, and corresponding fluorinated products after treatment with CHF_3

Oxide precursors			Fluorinated products			
Sample	**Al/Ga ratio**	**BET area, $m^2\ g^{-1}$**	**Sample**	**Fluorination temperature, K**	**BET area, $m^2\ g^{-1}$**	**Fluorine content, wt.% F^-**
Al#0	/	235	Al#01-F	473	190	1.9
			Al#02-F	523	192	3.4
			Al#03-F	573	170	7.4
			Al#04-F	623	130	18.8
			Al#05-F	673	58	34.1
			Al#06-F	723	21	46.0
Ga#0	/	87	Ga#01-F	473	89	0.52
			Ga#02-F	523	86	1.1
			Ga#03-F	573	82	2.1
			Ga#04-F	623	79	3.6
			Ga#05-F	673	74	4.7
			Ga#06-F	723	55	10.9
Al/Ga-100	100	200	Al/Ga-100-F	623	120	16.3
Al/Ga-50	50	207	Al/Ga-50-F	623	108	15.3
Al/Ga-25	25	220	Al/Ga-25-F	623	119	15.1
Al/Ga-15	15	250	Al/Ga-15-F	623	147	21.8
Al/Ga-5	5	210	Al/Ga-5-F	623	171	19.8
Al/Ga-2	2	296	Al/Ga-2-F	623	155	16.9
Al/Ga-1	1	164	Al/Ga-1-F	623	139	9.8

des) with a heating rate of 2 K min^{-1}. Evolution of pyridine was monitored by on-line FTIR spectroscopy; thermally treated solid materials were examined by PA-FTIR spectroscopy.

Surface area determination: Specific surface areas were determined with a FlowSorb II 2300 instrument (Micromeritics) using a single-point BET method and N_2 adsorption at 77 K. Before each analysis, solid samples were evacuated at 523 K for several hours and additionally conditioned at the same temperature under flow of N_2 for 1 h in the test tube of the FlowSorb instrument.

3 Results and Discussion

3. 1. General Characteristics of Oxide Precursors and Fluorinated Products

3. 1. 1. Oxide Precursors

Surface areas and denomination of single and mixed oxide xerogels used as precursors in the present study are presented in Table 1. Surface areas of single oxides differ considerably, 235 $m^2 g^{-1}$ for Al_2O_3 (Al#0) *vs.* 87 $m^2 g^{-1}$ for Ga_2O_3 (Ga#0). In general, this divergence is consistent with previous comparative studies where it was found that surface areas of γ-Ga_2O_3 are always considerably lower, usually up to two times, as those of similarly prepared γ-Al_2O_3 analogues, *e.g.* respective ranges reported for γ-Ga_2O_3 and γ-Al_2O_3 are 100–160 $m^2 g^{-1}$ and 170–300 $m^2 g^{-1}$.[2,4–7] Surface area of Al#0 is within the typical values for γ-Al_2O_3, while that of Ga#0 is somehow lower as reported for γ-Ga_2O_3. In previous studies, Ga_2O_3 materials with surface areas below 100 $m^2 g^{-1}$ were found to be at least partially crystallised;[3,6,30] *e.g.* inorganic preparation route, similar to that used in the present study, yielded crystalline α-Ga_2O_3 with surface area of 77 $m^2 g^{-1}$.[30] According to these precedents, relatively low surface area of Ga#0 could be associated with the formation of crystalline Ga_2O_3 phases. XRD measurements do however not give any evidence for that and show that both single oxides, Al#0 and Ga#0, are of very low crystallinity and consist only of metastable γ-Al_2O_3 and γ-Ga_2O_3 phases.

Mixed oxides investigated within this study comprise a series of Al_2O_3/Ga_2O_3 xerogels with Al_2O_3:Ga_2O_3 ratios ranging from 100:1 (Al/Ga-100) to 1:1 (Al/Ga-1). Nominal compositions, denomination and surface areas of mixed xerogels are given in Table 1. Surface areas of the mixed xerogels with lower Ga_2O_3 contents, up to the sample Al/Ga-2, are within the range typically observed for γ-Al_2O_3 (Al#0). Only the xerogel with the highest Ga_2O_3 content, Al/Ga-1, exhibits a lower surface area of 164 $m^2 g^{-1}$. As reported, surface area of mixed γ-Al_2O_3/γ-Ga_2O_3 is decreasing steadily with increasing γ-Ga_2O_3 content;[4,6,7,31] there is however also a number of reports where no distinctive trends were observed.[5,8,20,24] XRD patterns of representative mixed Al_2O_3/Ga_2O_3 xerogels are shown in Fig. 1 (traces a, c and e). Corresponding patterns are very similar to those of single oxides, γ-Al_2O_3 and γ-Ga_2O_3 (not shown). Broadness and low intensity of diffraction lines indicate that crystallinity is low what is in line with the observed high surface area of all mixed xerogels. Mixed γ-Al_2O_3/γ-Ga_2O_3 are commonly described as solid solutions with spinel-type structure.[4–7,31] Most indicative feature of these solutions is the enlargement of the unit cell parameter of γ-Al_2O_3 when Al^{3+} ions are isomorphically substituted by larger Ga^{3+} ions. This is manifested by the shift of characteristic diffraction lines to lower diffraction angles. Such shifts with increasing Ga_2O_3 contents are clearly observed also for current mixed oxides, as seen in Fig. 1 for the two typical lines of γ-Al_2O_3 at 45.6 and 66.6°, indicating the formation of γ-Al_2O_3/γ-Ga_2O_3 solid solutions.

3. 1. 2. Fluorinated Products

Fluorination of single oxides with CHF_3 under flow conditions was studied in the temperature range of 473–723 K (Table 1). For both single oxides, extent of fluorination deduced from the fluorine content of fluorinated products strongly depends on the temperature and is considerably higher for the γ-Al_2O_3-based Al#0 than for the γ-Ga_2O_3-based Ga#0.

Fluorination of a series of mixed oxides was carried out at intermediate temperature of 623 K. Extent of fluorination for the mixed xerogels is close to the value found for the γ-Al_2O_3-based Al#0 treated at the same temperature (Table 1, sample Al#04-F). Within mixed xerogels, distinctively lower fluorine content is observed only for the Ga_2O_3-rich sample, Al/Ga-1. This implies that fluorination processes are not affected by intermediate levels of Ga. Another noticeable effect of fluorination is the decrease of surface area observed for all fluorinated oxide precursors. Corresponding reductions in surface areas are proportional to the extent of fluorination, as evidenced by the Al#0 and Ga#0 fluorination experiments performed at different temperatures (Table 1). Similar effects of fluorination were observed for a number of γ-Al_2O_3 and related materials and were usually associated with the expansion and crystallisation processes that take place during the conversion of the oxide matrix to bulk fluoride phase(s).[11,12,18,19]

Chemical analysis indicates that all oxide xerogels underwent fluorination, although to different extents, *e.g.* Al#0 and Ga#0 fluorinated at 623 K contain, respectively, an equivalent of 27.7 wt.% of AlF_3 (Al#04-F) and 8.0 wt.% of GaF_3 (Ga#04-F). XRD investigations of fluorinated materials, performed shortly (within few days) after fluorination, do not reveal any crystalline phase(s), as exemplified on Fig. 1 (trace f) for the Al/Ga-1-F sample. Recorded XRD patterns remain practically identical to those of the γ-Al_2O_3 and/or γ-Ga_2O_3 precursors. In an earlier study, no crystalline phases were detected in fluorina-

ted γ-Al_2O_3 containing up to 68 wt.% of AlF_3.[11] It was concluded that even at such high AlF_3 contents fluoride remains strongly dispersed and of very low crystallinity that can not be detected by XRD. It is very likely that similar fluoride phases, amorphous to X-rays, were formed also here, especially in Ga-rich materials where the extent of fluorination is lower. Further XRD investigations, performed within several months after preparation, showed however that the initial amorphous fluoride phases are not stable. Although the materials were stored and manipulated under dry conditions, noticeable crystallisation occurred, as shown in Fig. 1 (traces b, d and g) for the three representative fluorinated mixed xerogels. Besides the unconverted oxide phase, XRD indicates the formation of a crystalline hydrated aluminium hydroxyfluoride with general formula, $Al(F,OH)_3{\cdot}nH_2O$, having a pyrochlore structure and not well-specified composition.[32] Comparison with the XRD data from a previous study of Al-hydroxyfluorides[33] indicates that the crystallised product closely matches the compound with the reported composition of $AlF_{1.7}(OH)_{1.3}{\cdot}H_2O$. Crystallisation of hydrated AlF_3 or hydroxyfluoride phases after exposure to ambient air was also noticed in some previous reports dealing with amorphous AlF_3 with unusually high surface areas.[34–36] These findings gave clear evidence that H_2O uptake in these materials can be substantial, as anticipated from their strong Lewis acidity and high surface area. Recent *ab initio* and XPS investigations of AlF_3 with high surface areas,[36] substantiated by computed phase diagrams for AlF_3 surfaces,[37] strongly suggest that at room temperature H_2O adsorption followed by surface hydroxylation, hydration and hydrolysis can be very significant, and, more importantly, that these processes take place already at H_2O levels that are orders of magnitude lower than those practically achievable in the laboratory, even if all operations are carried out at thoroughly controlled dry conditions. It is therefore very likely that formation of crystalline hydrated phases observed for the current partially fluorinated oxides is the result of H_2O adsorption during manipulation and storage that can practically not be avoided, as mentioned above. For the fluorinated mixed oxides, shown in Fig. 1, it is clear that the extent of crystallisation of the $Al(F,OH)_3{\cdot}nH_2O$ phase is inversely proportional to the Ga content. It should be noted that for the fluorinated single Ga_2O_3 (sample Ga#06-F, not shown) post-crystallisation was also observed. In fluorinated mixed oxides, behaviour of Ga is therefore different; preferential crystallisation of Al-hydroxyfluoride indicates that Ga-phases are not involved in the bulk crystallisation processes. Contrarily, they apparently retard the crystallisation of Al-rich phases, probably by lowering the concentration of available Al-species. On the other side, preferential formation of crystalline $Al(F,OH)_3{\cdot}nH_2O$ phases may lead to the formation of segregated Al- and Ga-rich regions that may considerably increase the heterogeneity of these materials on a macro scale.

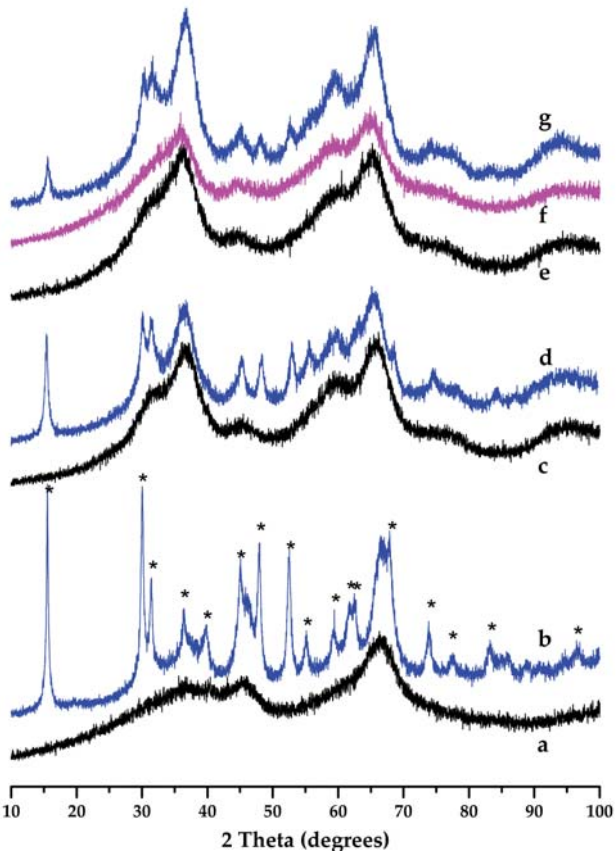

Figure 1. Representative powder diffractograms (offset) for mixed oxide precursors and products of fluorination with CHF_3 at 623 K; Oxide precursors: (a) Al/Ga-100, (c) Al/Ga-2, and (e) Al/Ga-1; Fluorinated products: (b) Al/Ga-100-F (aged), (d) Al/Ga-2-F (aged), (f) Al/Ga-1-F (fresh), and (g) Al/Ga-1-F (aged). Corresponding compositions are given in Table 1. * – $Al(F,OH)_3{\cdot}nH_2O$[32]

Thermal behaviour of fluorinated products was verified with temperature programmed (TP) experiments, performed up to 773 K in flow of N_2. Effluent gases were monitored by on-line FTIR spectroscopy; representative evolution profiles for HF and H_2O for the Al/Ga-100-F sample are shown in Fig. 2. Similar HF evolution profiles were recorded for the $MF_{3-x}(OH)_x{\cdot}nH_2O$ (M=Al or Ga) type of compounds[38] and for fluorinated Ga-doped Al_2O_3[21]. Current TP experiments show that H_2O desorption from the fluorinated products is substantial. Inverse course of H_2O and HF evolution profiles is a clear indication that hydrolysis of the fluoride phase is taking place. According to TP experiments, current fluorinated oxides are relatively stable towards hydrolysis at temperatures below 500 K, above this temperature, and especially above 650 K, all treatments performed under non-fluorinating conditions will led to some defluorination. As found for very active AlF_3-based materials, their surface and bulk properties may be strongly altered by hydration and hydrolysis.[36,39] Such effects are expected to be less pronounced for current partially fluorinated oxides that already

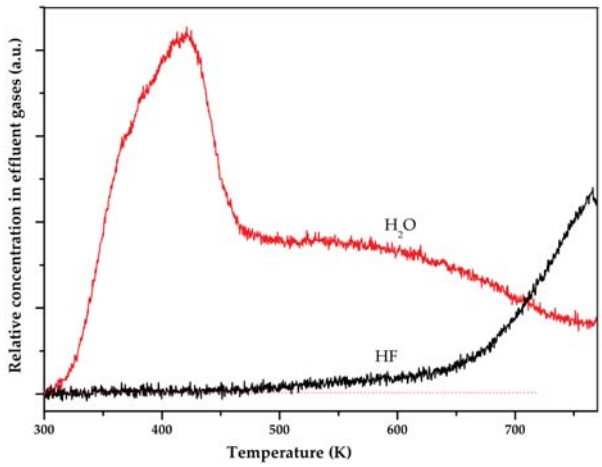

Figure 2. H_2O- and HF-evolution profiles obtained with a temperature programmed heating of Al/Ga-100-F in flow of N_2.

consist of mixed bulk oxide/hydroxyfluoride phases, *i.e.* phases that are formed during the hydrolysis of stoichiometric fluorides.

3. 2. XPS Investigations

XPS was applied in order to get insights into surface chemistry of samples Ga#0, Al/Ga-1 and Al/Ga-2 before and after treatment with CHF_3. The sample Al/Ga-15 was measured by XPS only after treatment with CHF_3 (Al/Ga-15-F). Surface concentrations were calculated from the XPS spectra and are given in Table 2. As it can be seen, carbon is present on the surface of all samples probably due to adventitious carbon species related with the exposure of samples to air atmosphere. Surface composition of the oxide precursors is roughly consistent with their nominal composition, *i.e.* concentration of Al on Al/Ga-2 is approximately two times higher than on sample Al/Ga-1. After treatment with CHF_3 all samples contain F. The highest concentration of F, ~35 at.%, was found on the Ga#4-F sample. Treatment of mixed Al/Ga-oxides with CHF_3 resulted in lower F concentrations which were about 13 at.%. Incorporation of F is accompanied by a clear decrease of surface O concentrations. This reflects the reaction of substitution of oxygen atoms by fluorine atoms.

Interesting parameter which was changing during CHF_3 treatment is the ratio between surface Al and Ga atoms (Table 2). As expected, the Al/Ga ratio for the mixed oxide Al/Ga-2 is about two times higher than for Al/Ga-1. However, comparison of nominal and measured Al/Ga ratios shows that surfaces of mixed oxides are enriched with Al. Similar results were also obtained in some related studies.[7,24] This suggests that in mixed Al/Ga-oxides surface relaxation and reconstruction processes are very likely cation-specific. Inverse process was observed after treatment with CHF_3; the Al/Ga ratio decreased nearly by factor of two with respect to the un-treated mixed oxides. This means that surfaces of CHF_3-treated oxides are enriched by Ga with respect to Al. At the same time the F/Al ratios (Table 2) remain very similar for all three samples analysed. These observations can be interpreted as formation of the Al–F based phases in the subsurface region what lefts Ga–O phases enriched on the surface.

In order to understand chemical bonding at sample surfaces before and after CHF_3 treatment, high resolution XPS spectra were acquired which are presented in Fig. 3 for Ga#0 and Ga#04-F, and in Fig. 4 for Al/Ga-1 and Al/Ga-1-F. XPS results show that fluorination of pure Ga_2O_3, Ga#0 sample, leads to two types of Ga chemical environments, Ga_2O_3 and Ga–F (Figs. 3a and 3b). This was recognised from the Ga 2p and Ga 3d spectra. On pure Ga_2O_3 sample Ga 2p is at 1118.0 eV and Ga 3d is at 20.0 eV. Energy of 20.0 eV for the Ga 3d peak is characteristic of Ga^{3+} oxidation state, what can be expected for Ga_2O_3.[28,40] After fluorination new peaks appear in addition to previous ones: in Ga 3d spectrum at 22.0 eV and in Ga $2p_{3/2}$ spectrum at 1119.5 eV. These new peaks can be related with the formation of Ga–F bonds, as suggested in literature.[40,41] This shows that partial fluorination of Ga_2O_3 occurred, what follows also from appearance of F at the surface (Table 2). On fluorinated Ga#04-F, F 1s spectrum (Fig. 3d) is asymmetric towards low binding energy side. This can be interpreted as a presence of two peaks at 686.5 eV and 684.0 eV indicating two types of F-sites. In literature the

Table 2. Surface concentration (in at.%) determined by XPS for the analysed oxide precursors and fluorinated products

Sample	Surface concentration, at.%					Al/Ga (nominal / measured)	F/Al
	C	O	Ga	Al	F		
Ga#0	37.4	45.5	17.2	–	-	–	–
Ga#04-F	27.6	20.6	17.1	–	34.9	–	–
Al/Ga-1	31.2	48.3	7.8	12.7	–	1 / 1.6	–
Al/Ga-1-F	15.1	40.0	16.7	15.7	12.7	1 / 0.9	0.81
Al/Ga-2	19.2	55.9	7.0	20.3	-	2 / 2.9	–
Al/Ga-2-F	20.6	41.5	9.1	16.2	12.7	2 / 1.8	0.78
Al/Ga-15-F	18.9	43.5	2.1	17.6	13.4	15 / 8.6	0.76

main peak is attributed to fluoride species and the second peak to different F/O environments, where the presence of O causes redistribution of electron density.[19] Oxygen O 1s spectra show broad structure with a maximum at around 531.8 eV. This is related with oxygen atoms bound in oxide matrix. The O 1s spectra are also asymmetric towards higher binding energy (532–533 eV), what is characteristic for hydroxides and adsorbed water.

spectra is that peaks at 22.0 eV and at 1119.5 eV, observed in Ga 2p and Ga 3d spectra of the CHF_3-treated Ga_2O_3 (Ga#04-F in Figure 3), are not present. This indicates that Ga-atoms in mixed oxides are not involved to a greater extent in direct interactions with F. Ga 3d peak at 20.0 eV is characteristic for the Ga^{3+} oxidation state in oxides. In addition, XPS does not reveal any reduction to $Ga^{<3+}$ states, presence of the latter should be recognised as a shift in

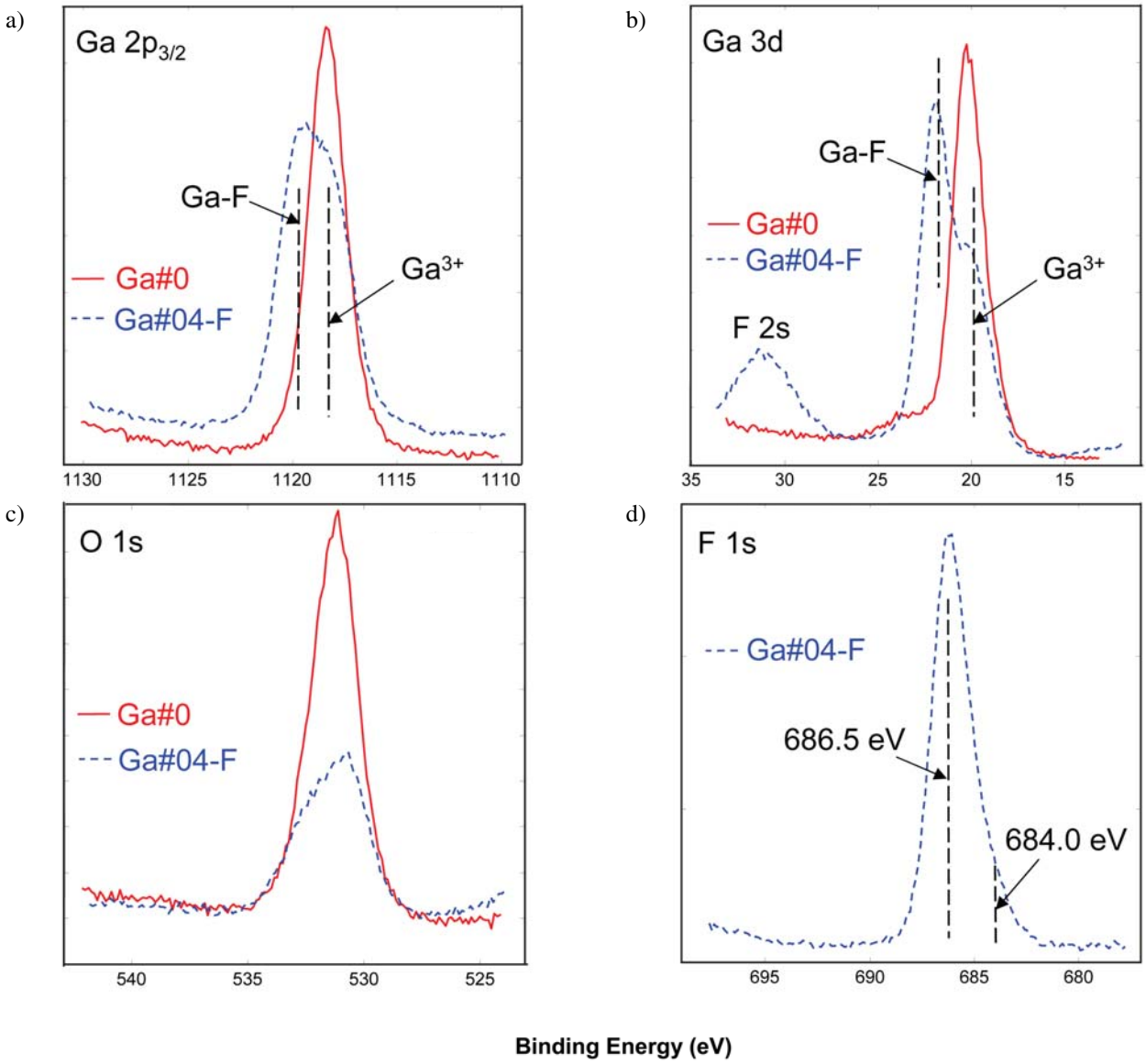

Figure 3. XPS spectra of Ga 2p (a), Ga 3d (b), O 1s (c) and F 1s (d) for γ-Ga_2O_3 (Ga#0) and its fluorinated product (Ga#04-F). Y-axes present photoemission intensities.

Similar XPS characterisation was performed on representative mixed oxides. XPS spectra of Al/Ga-1 and Al/Ga-2 were quite similar. Only XPS spectra of Al/Ga-1 before and after fluorination with CHF_3 are therefore shown in Fig. 4. The most noticeable feature of these

XPS spectra towards lower binding energies.[28,40] XPS spectrum of Al 2p is shown in Fig. 4e. The main peak Al 2p is at 74.0 eV what is characteristic for Al^{3+} in oxides.[28] Small shift towards higher binding energy of Al 2p peak of 0.5 eV was only observed after fluorination which may

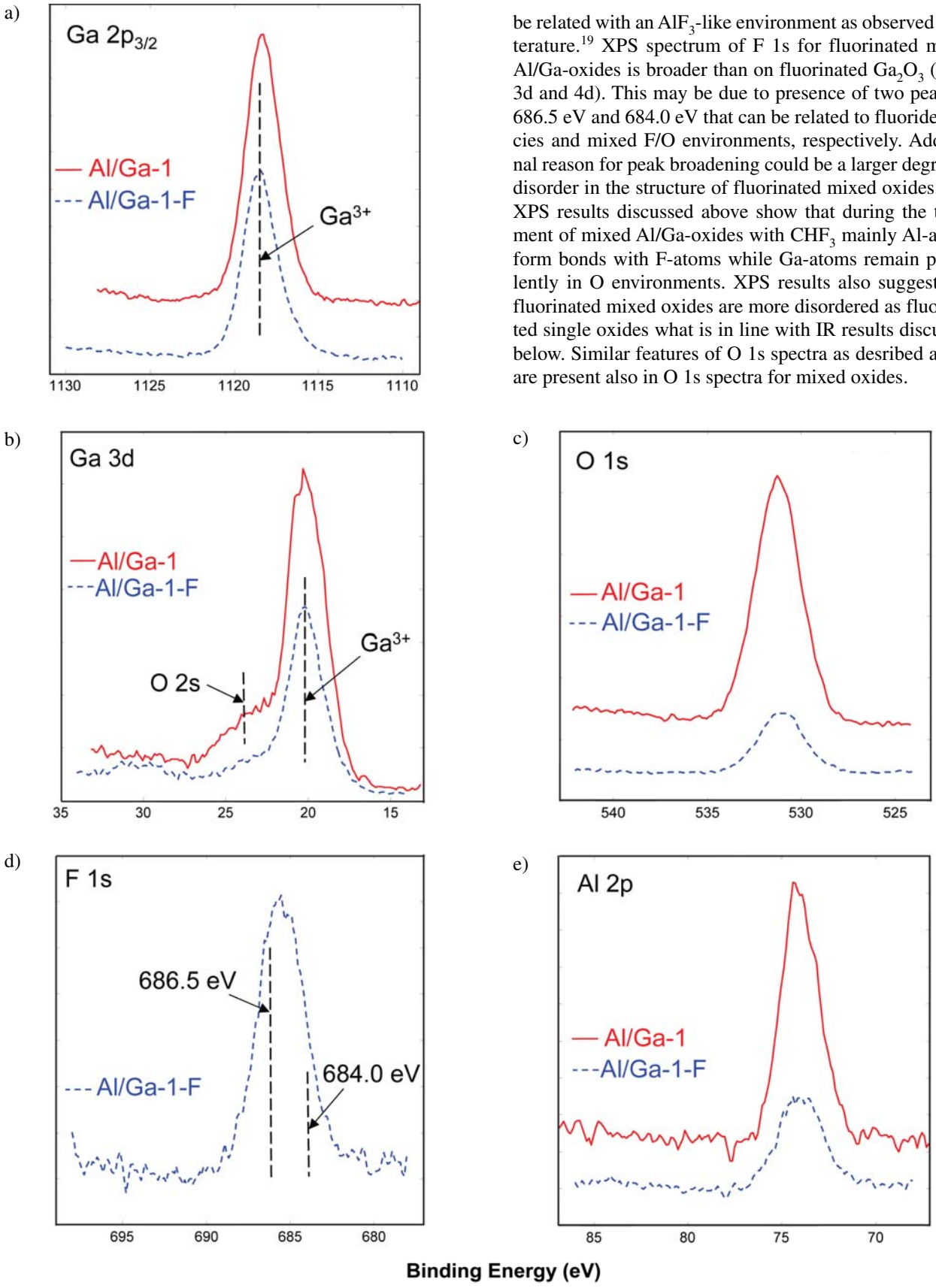

Figure 4. XPS spectra of Ga 2p (a), Ga 3d (b), O 1s (c), F 1s (d) and Al 2p (e) for mixed oxide (Al/Ga-1) and its fluorinated product (Al/Ga-1-F). Y-axes present photoemission intensities.

be related with an AlF_3-like environment as observed in literature.[19] XPS spectrum of F 1s for fluorinated mixed Al/Ga-oxides is broader than on fluorinated Ga_2O_3 (Figs. 3d and 4d). This may be due to presence of two peaks at 686.5 eV and 684.0 eV that can be related to fluoride species and mixed F/O environments, respectively. Additional reason for peak broadening could be a larger degree of disorder in the structure of fluorinated mixed oxides. Our XPS results discussed above show that during the treatment of mixed Al/Ga-oxides with CHF_3 mainly Al-atoms form bonds with F-atoms while Ga-atoms remain prevalently in O environments. XPS results also suggest that fluorinated mixed oxides are more disordered as fluorinated single oxides what is in line with IR results discussed below. Similar features of O 1s spectra as desribed above are present also in O 1s spectra for mixed oxides.

3. 3. Surface Properties Investigated by Pyridine Adsorption

Pyridine, a relatively hard Lewis base with rather high chemical stability, is a classical IR probe to determine the acidity of Al_2O_3-based materials[42] as well as that of their fluorinated analogues with largely different AlF_3 contents[16,43]. In the present study, spectroscopic investigations of adsorbed pyridine were used to follow the changes in acidity within the series of mixed oxides, and after fluorination. Indicative PAS-py spectra of oxide precursors and related fluorinated products are presented in Figs. 5a and 5b, respectively.

3. 3. 1. PAS-py of Oxide Precursors

PAS-py spectra of the two single oxides, Al#O and Ga#0 in Fig. 5a, are characterised by the bands at about 1450, 1491, 1579 and 1615 cm^{-1}, that are typically assigned to pyridine coordinatively bonded to Lewis acid sites.[16] Absence of any significant bands at around 1545 and 1640 cm^{-1} indicates that strong Brønsted acid sites, capable to protonate pyridine to pyridinium species, are not present. In general, these results are consistent with previous reports on the acidity of amorphous γ-Al_2O_3 and γ-Ga_2O_3 where pyridine adsorption revealed only the presence of relatively strong Lewis acid sites.[2,7,16,30]

PAS-py spectra of some representative mixed oxides are shown in Fig. 5a. Main bands of adsorbed pyridine remain at approximately the same positions as in single oxides, at 1493, 1579 and 1615 cm^{-1}; only the band at 1447 cm^{-1} in Al#0 is blueshifted to 1450 cm^{-1}. However, intensity of all bands associated with Lewis acid sites is increasing with increasing Ga content. In addition, appearance of two new bands, observed as shoulders at 1458 and 1621 cm^{-1}, is evident for mixed oxides with higher Ga contents, starting from Al/Ga-5 upwards (Fig. 5a). All these findings suggest that acidity of current γ-Al_2O_3/γ-Ga_2O_3 xerogels is higher than that exhibited by individual oxides, as noted in a number of previous studies.[4,7,8,44,45] Current results suggest that although the strength of the Lewis

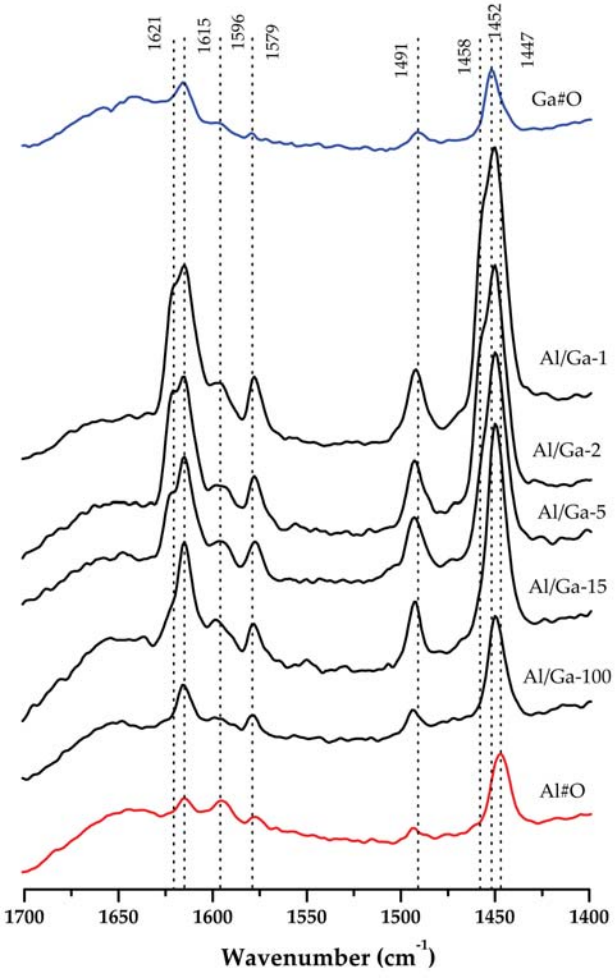

Figure 5a. PAS-py absorbance spectra (offset) of oxide precursors after pyridine adsorption at 423 K.

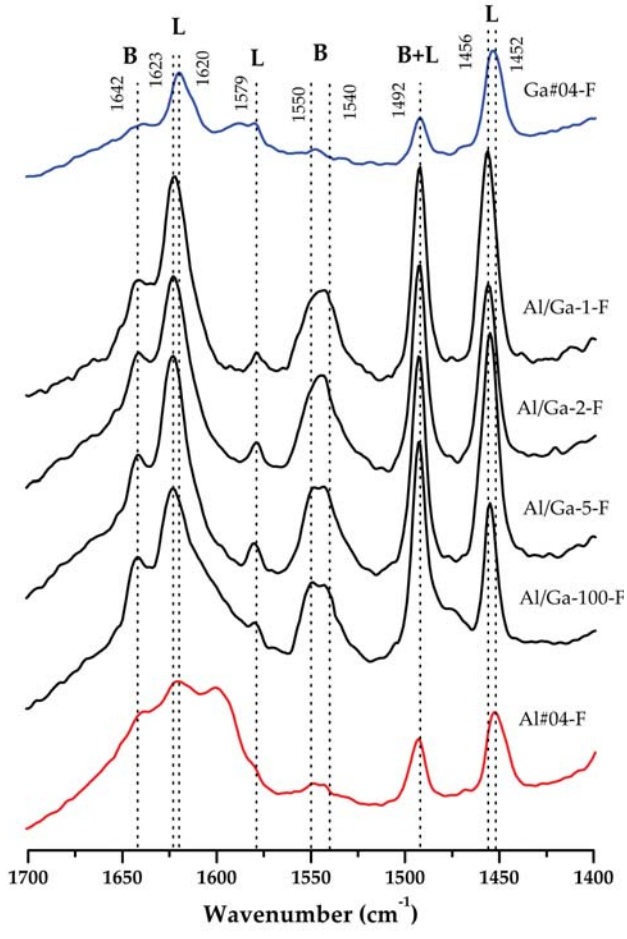

Figure 5b. PAS-py absorbance spectra (offset) of oxides fluorinated with CHF_3 at 623 K after pyridine adsorption at 423 K. Bands of pyridine adsorbed on Lewis and Brønsted acid sites are marked with L and B, respectively.

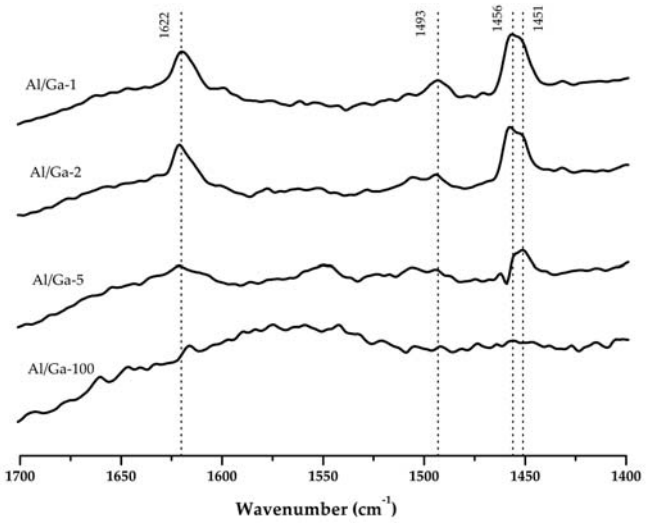

Figure 6a. PAS-py absorbance spectra (offset) of representative mixed oxide precursors; pyridine adsorbed at room temperature and desorbed in flow of N_2 at 673 K.

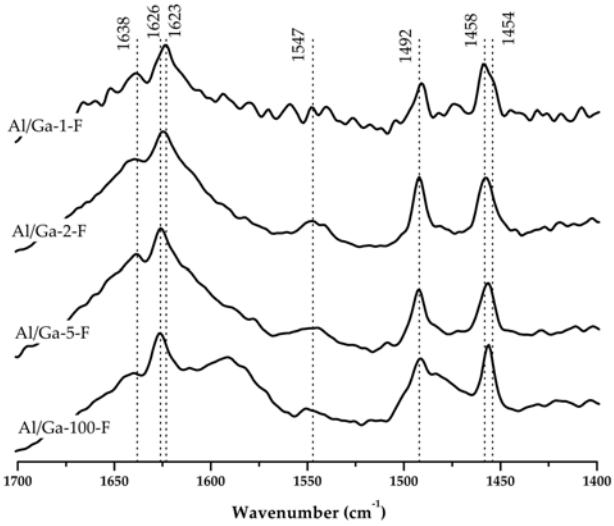

Figure 6b. PAS-py absorbance spectra (offset) of representative mixed oxides fluorinated with CHF_3 at 623 K; pyridine adsorbed at room temperature and desorbed in flow of N_2 at 623 K.

acid sites remains apparently the same, their number is increasing with increasing Ga content and at the highest Ga contents studied (Al/Ga ratios from 5 to 1) additional Lewis acid sites, presumably with higher strength, are formed. The latter presumption is supported by PAS-py spectra recorded after heating the mixed oxides with pre-adsorbed pyridine to 673 K. As shown in Fig. 6a, at 673 K pyridine is retained only on samples with higher Ga contents, *i.e.* samples Al/Ga-(1–5). Corresponding spectra are characterised by a doublet at 1451/1456 cm^{-1} and a single band at 1622 cm^{-1} suggesting the presence of Lewis acid sites with higher strength, such sites are evidently not present in mixed oxides with lower Ga contents, *e.g.* sample Al/Ga-100 in Fig. 6a, which, after heating to 673 K, do not show any pyridine retention.

Lewis acidity of Al_2O_3 and Ga_2O_3 is in general associated with the presence of coordinatively unsaturated (cus) Al^{3+} or Ga^{3+} cations on the surface; the strongest acid sites being those originating from tetrahedral cus cations, cus-Al^{IV} and cus-Ga^{IV}.[2,30,31,42] Lewis acidity of surface cus-Ga^{IV} sites in γ-Ga_2O_3 was found to be weaker than that of the corresponding cus-Al^{IV} in γ-Al_2O_3.[2] In the same study, density of acid sites on γ-Ga_2O_3 was higher than that on γ-Al_2O_3, presumably due to a higher tetrahedral preference of Ga^{3+} vs. Al^{3+} resulting in a higher concentration of strongly acidic cus-Ga^{IV} on γ-Ga_2O_3. In analogy with single oxides, Lewis acidity of mixed γ-Al_2O_3/γ-Ga_2O_3 is related to the presence of both types of acidic sites, cus-Al^{IV} and cus-Ga^{IV}.[7,31,44] However, due to the already mentioned preference of Ga^{3+} ions to occupy tetrahedral positions, there are no direct correlations between actual Al^{IV}/Ga^{IV} ratios and nominal Al/Ga ratios derived from the composition of γ-Al_2O_3/γ-Ga_2O_3 solid solutions. NMR[7,31] and EXAFS/XANES[3,4] investigations gave a strong evidence that in these solid solutions majority of available tetrahedral positions is occupied by Ga^{3+} ions while Al^{3+} ions prevalently reside in octahedral positions. According to NMR investigations, in a solid solution with the nominal Al/Ga ratio of 1/1 (a direct equivalent to the current Al/Ga-1 sample) the Al^{IV}/Ga^{IV} ratio in the bulk is 1/2.88 vs. Al^{VI}/Ga^{VI} of 1/0.73.[31] On the other side, IR spectroscopy of adsorbed probe molecules, like CO or pyridine, that can give a reliable information on the type and number of surface acid sites, cannot make a clear distinction between surface sites specific for cus-Al^{IV} or cus-Ga^{IV}.[31,45] Similar low selectivity can be expected also for current γ-Al_2O_3/γ-Ga_2O_3, *e.g.* spectra of pyridine adsorbed on individual γ-Al_2O_3 and γ-Ga_2O_3 are very similar with the relevant bands of adsorbed pyridine being shifted only for few cm^{-1}.[2] In amorphous or poorly crystalline mixed oxides bands of adsorbed species are additionally broadened what can lead to a considerable overlap of individual components. This may result in partially resolved or completely non-resolved composite bands.

For γ-Al_2O_3, the band at ca. 1625 cm^{-1} is assigned to pyridine being adsorbed on cus-Al^{IV} sites that are considered to be the strongest Lewis acid sites found on the surface of transition aluminas.[42,46] By analogy, band at ca. 1622 cm^{-1} observed in current mixed oxides with higher Ga contents could tentatively be attributed to the appearance of cus-Ga^{IV} sites.[46] The reasons for the formation of such strongly acid sites only in Ga-rich samples are however not entirely clear. As reported before, strongly acidic cus-Al^{IV} sites are formed after γ-Al_2O_3 dehydration at relatively high temperatures, e.g. 773 K.[42] Absence of these sites in current oxides, clearly seen in Al-rich samples, can therefore be ascribed to the lower dehydration temperature, 723 K, used within this study. The fact that at the same

treatment temperature strongly acidic cus-Ga^{IV} sites are readily formed in Ga-rich samples can be, in part, attributed to the high preference of Ga for tetrahedral vs. octahedral coordination.[2,30] Probably more important, it appears that the preferentially formed cus-Ga^{IV} sites are efficiently stabilised within the mixed Al/Ga environments when Ga content is increasing. This assumption is somehow in line with a previous study of Ga_2O_3 supported on γ-Al_2O_3 where it was found that presence of the Al_2O_3 phase favours the formation of cus-Ga^{3+} sites.[44] In addition, increased Lewis acidity observed in Ga/Al-oxides was attributed to the formation of mixed Ga–O–Al linkages.[21] On the other side, it is known that observed concentration of the strongest cus-Al^{IV} sites on γ-Al_2O_3 is much lower than expected from its structural features, very likely due to surface reconstruction and ion-shielding effects;[42] in addition, DFT calculations suggest a spontaneous conversion of surface cus-Al^{IV} sites to quasi-bulk Al^{VI} sites with concomitant reduction in Lewis acidity.[47] It can be speculated that such reconstruction processes are apparently less effective for cus-Ga^{IV} sites in mixed Al/Ga environments what results in their higher retention on the surface. In contrast to the present results, spectra of adsorbed pyridine on a series of single and mixed Al_2O_3/Ga_2O_3 catalysts prepared by precipitation from alcoholic solutions do not exhibit any explicit double bands.[7] This indicates that composition and especially the structure of mixed γ-Al_2O_3/γ-Ga_2O_3 surfaces may strongly depend on specific preparation and post-treatment conditions employed in different preparative approaches.

Observed increase of overall acidity in mixed oxides strongly suggests that the structure of mixed γ-Al_2O_3/γ-Ga_2O_3 surfaces is much more heterogeneous than that of the single oxides, γ-Al_2O_3 and γ-Ga_2O_3. This is also supported by TPF experiments (see Section 3.4). Mixed γ-Al_2O_3/γ-Ga_2O_3 are not typical homogeneous solid solutions. Namely, due to the preferential occupation of tetrahedral positions by Ga, they already include some structural heterogeneity. In addition, bulk structure is rather complex and includes different possible environments, M–O–M (M=Al,Ga), and coordinations, $Al^{IV+V+VI}$ and Ga^{IV+VI},[31] that all depend on the specific Al/Ga ratio. Diversity of these bulk structural features is reflected on the surface increasing its complexity and heterogeneity in comparison with single oxides. Real structures of mixed surfaces are however not known, especially with respect to possible surface reconstruction processes. Reliable modelling of surface relaxation and reconstruction processes was apparently accomplished only for γ-Al_2O_3,[47] similar calculations for mixed γ-Al_2O_3/γ-Ga_2O_3 surfaces are still missing.

3. 3. 2. PAS-py of Fluorinated Products

PAS-py spectra of single and mixed oxides fluorinated with CHF_3 at 623 K are shown in Fig. 5b. In addition to bands associated with Lewis acid sites, located at 1453–1456, 1492, 1579 and 1620–1623 cm^{-1}, spectra also reveal bands at 1492, 1540–1550 and 1642 cm^{-1} that are characteristic for pyridine interacting with strong Brønsted acid sites. Close similarity of current spectra with those reported earlier for $CHClF_2$-fluorinated γ-Al_2O_3[16] indicates that both fluorinating agents, CHF_3 and $CHClF_2$, yield fluorinated products with very similar surface characteristics. This is somehow consistent with previous XPS investigations, where comparable fluorinating capabilities of both fluorocarbons towards γ-Al_2O_3 were observed; CHF_3 was however found to be more efficient than $CHClF_2$ in fluorinating a model γ-Al_2O_3 catalyst.[17] For the current fluorinated products, comparison of PAS-py spectra with those of corresponding oxide precursors (Fig. 5a) demonstrates that after fluorination all relevant bands associated with Lewis acidity, e.g. bands at around 1450 and 1615 cm^{-1}, are blueshifted. This is commonly explained by strengthening of Lewis acid sites through inductive effects due to the replacement of O- and OH-species with strongly electronegative F.[16] As is the case for mixed oxide precursors, bands of adsorbed pyridine in fluorinated mixed oxides are more intense and blueshifted, for approximately 3 cm^{-1}, with respect to fluorinated single oxides. This suggests that both, the number and the strength of Lewis acid sites, of fluorinated mixed oxides are higher. In addition, double bands observed in Ga-rich mixed oxides disappear after fluorination, suggesting a partial reduction in heterogeneity of the Lewis acid sites. Increased acidity after fluorination is confirmed also by PAS-py spectra after pyridine desorption at 623 K. Related spectra are shown on Fig. 6b. As expected, such treatment considerably reduces the Brønsted acidity and reveals the presence of strong Lewis acid sites with corresponding bands positioned at 1456–1458 and 1623–1626 cm^{-1}. In comparison with the similarly treated mixed oxides (Fig. 6a), fluorinated Ga-rich mixed oxides exhibit only a slight blueshift of 1–2 cm^{-1}, indicating a relatively low effect of fluorination on acidity. On the other side, Al-rich samples, which as oxides do not show any considerable Lewis acidity, in their fluorinated form exhibit the presence of strong Lewis acid sites; most notable is the occurrence of the band at 1626 cm^{-1}. Position of this band is close to the band at 1628 cm^{-1} found in $AlF_{2.6}(OH)_{0.4}{\cdot}nH_2O$ (n=0.1–0.2)[48] and band at 1627 cm^{-1} for $AlF_{3-x}(OH)_x$-type of compounds[49]. For these compounds with hexagonal tungsten bronze (HTB) structure the indicated bands were associated with the presence of very strong Lewis acid sites related to cus-Al^{3+} ions. It is therefore reasonable to conclude that in the current fluorinated Al-rich samples strong Lewis acid sites originate prevalently from cus-Al^{3+} ions in various O/F environments. In Ga-rich samples, concentration of strong cus-Al^{3+} sites is lower due to the preferential formation of cus-Ga^{3+} ions which in turn exhibit lower Lewis acidity.[2] In addition, pyridine adsorption on HTB hydroxyfluorides of the type, $MF_{3-x}(OH)_x{\cdot}nH_2O$ (M=Al or Ga), revea-

led a higher Lewis acid strength of the Al-containing compound.[38]

It should also be mentioned that besides the observed increase of Lewis acid strength, fluorination apparently lowers the heterogeneity of these surface sites, as suggested by the disappearance of double bands and by band narrowing. PAS-py spectra of mixed oxides (Fig. 5a) show that the width of the bands related to Lewis acid sites is increasing with increasing Ga-content, *i.e.* full width at half maximum (FWHM) of the band at ca. 1452 cm^{-1} is increasing from 10 cm^{-1} for Al/Ga-100 to 15 cm^{-1} for Al/Ga-1. This can be correlated with the formation of various new acid sites in Ga-rich oxides, as mentioned above. Observed FWHM of the corresponding bands in fluorinated oxides (Fig. 5b) is lower, *i.e.* 7 cm^{-1} for Al/Ga-100-F and 10 cm^{-1} for Al/Ga-1-F. Relative narrowing of these bands after fluorination indicates that some structure reconstruction and ordering is probably taking place, although at levels that are, at least in the initial stages, not detectable by XRD (Fig. 1, trace f). Namely, a recent TEM study clearly demonstrated that AlF_3-based materials, despite being completely amorphous to X-rays, may contain well-ordered regions consisting of nanocrystalline fluoride phases.[35]

3. 4. Temperature Programmed Fluorination (TPF) with CHF_3

A series of TPF experiments up to 673 K were performed to compare reactivities of single and mixed oxide towards CHF_3 in the initial stages of fluorination, *i.e.* when the reaction is limited mainly to the surface. Progress of fluorination was monitored by FTIR spectroscopy; corresponding CO evolution profiles are presented in Fig. 7. The two single oxides, samples Al#0 and Ga#0, start to react with CHF_3 at approximately 450 and 500 K, respectively. For the mixed oxides, onset of fluorination is similar to Al#0, reaction starts at approximately 450 K; sample with highest Ga-content (Al/Ga-1) being a clear exemption reacting already at 400 K. Most notable difference between single and mixed oxides is exhibited in the intermediate temperature region, 400–600 K, where mixed oxides show a higher and graduated CO evolution that roughly increases with increasing Ga-content. Intense CO evolution, observed for all investigated materials above 580–620 K, can be associated with the beginning of bulk fluorination processes. There are however no clear correlations between these temperatures and fluorine contents obtained in preparative fluorination runs at 623 K (Table 1). This suggests that bulk fluorination of the oxide matrix above 580–620 K is very likely controlled by diffusion. As shown before, fluorination of oxides is usually accompanied by a considerable decrease of internal porosity what may strongly affect diffusion processes within the particles of reacting solids.[11,12,18]

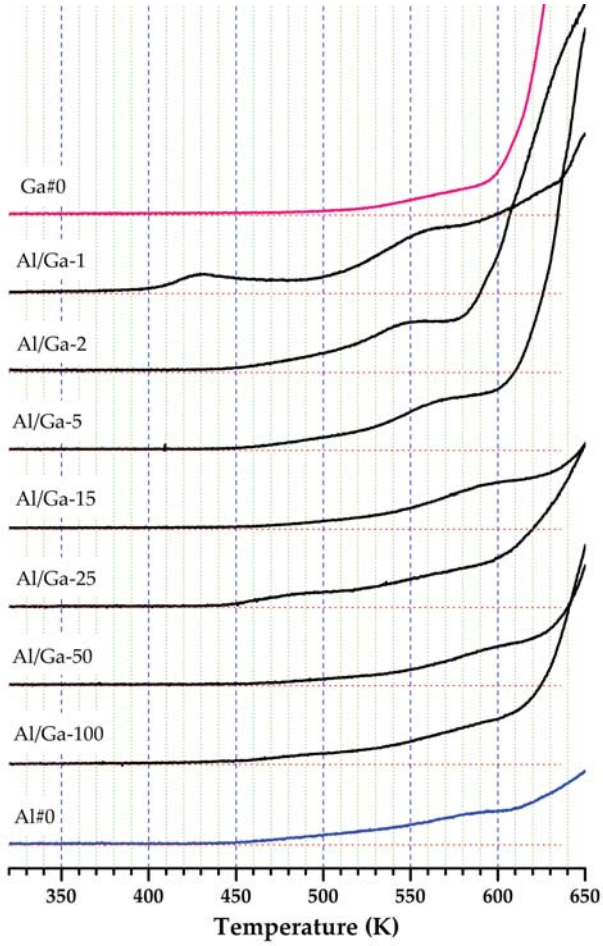

Figure 7. Temperature programmed reaction of single and mixed oxides with CHF_3 under flow conditions; corresponding CO-evolution profiles (offset) are shown.

TPF experiments clearly demonstrate that mixed oxides exhibit higher surface reactivity towards CHF_3 than the single oxides and that the reactivity is increasing with increasing Ga content. Very reactive surface sites in mixed oxides, capable to react with CHF_3 at 400–600 K, seem to be more abundant and differ from those present on single oxides. This is in good correlation with current PAS-py and XPS results (see above) that suggest a higher surface heterogeneity in mixed oxides, especially those with higher Ga contents. Surfaces with higher degree of heterogeneity are expected to exhibit higher concentration and broader variety of reactive surface sites. Within this study, the exact nature of these reactive sites could not be unequivocally determined. However, we recently found that the relatively stable CHF_3 molecule starts to react with solid alkali hydroxides at moderate temperatures, i.e. with KOH at 370 K and with NaOH at 420 K. Reactivity of these solids towards CHF_3 was, in the initial stages, ascribed to acid–base type of interactions between CHF_3 acting as a weak C–H acid and strongly basic oxygen species on the solid hydroxides.[27] In addition, in a previous

study of γ-Al_2O_3 fluorination it was clearly demonstrated that fluorination starts on basic OH groups.[15] Initial reactivity of current oxides towards CHF_3 can be therefore tentatively ascribed to similar interactions, probably involving different types of strongly basic surface sites, *e.g.* basic OH groups and possibly surface O^{2-} anions. In addition, observed higher reactivity of mixed oxide is consistent with earlier studies that demonstrated a higher basic character of γ-Ga_2O_3 w.r.t. γ-Al_2O_3,[2] and an increase of basicity for Ga_2O_3 supported on Al_2O_3 in comparison with individual oxide components.[45,50] We can therefore speculate that graded CO evolution is an indication of CHF_3 reactions with different types of strongly basic sites that are characteristic only for mixed γ-Al_2O_3/γ-Ga_2O_3 surfaces. Strong basic sites on such materials could possibly be probed by means of TPF with CHF_3. Further investigations are however required to verify these possibilities.

3. 5. Catalytic Behaviour in Isomerisation of CCl_2FCClF_2

Isomerisation of CCl_2FCClF_2 with subsequent dismutation reactions is frequently used as a model catalytic reaction to complement spectroscopic and other methodologies to evaluate the acidity of metal fluoride catalysts.[10,19,39,51,52] A number of such studies was carried out on AlF_3-based catalysts what allowed rather consistent comparisons between these solids, although their origin and characteristics varied significantly.[19,51] Accumulated data strongly suggest that on these solids isomerisation of CCl_2FCClF_2 to the thermodynamically preferred isomer, CCl_3CF_3, is facile and occurs via an intramolecular mechanism on medium strong or strong Lewis acid sites (Eq. 1).[10,39,51,52] Isomerisation is accompanied by consecutive dismutation processes involving CCl_3CF_3 (Eq. 2) and CCl_2FCF_3 (Eq. 3) with the latter being less facile than the former. Formation of $CClF_2CF_3$ is therefore observed only with very active catalysts and at higher temperatures,[13,19] as observed also in this study (Table 3).

$$CCl_2FCClF_2 \rightarrow CCl_3CF_3 \quad (1)$$

$$2CCl_3CF_3 \rightarrow CCl_2FCF_3 + CCl_3CClF_2 \quad (2)$$

$$2CCl_2FCF_3 \rightarrow CClF_2CF_3 + CCl_3CF_3 \quad (3)$$

Results of CCl_2FCClF_2 isomerisation tests performed on fluorinated single oxides and two representative mixed oxides are summarised in Table 3. For both fluorinated Al-rich oxides, single Al#04-F and mixed Al/Ga-100-F, catalytic behaviour is very similar indicating that catalytic functionality is not altered to a greater extent at low Ga levels. However, a slight reduction in catalytic activity, characterised by a slightly lower CCl_3CF_3 yields and considerably lower $CClF_2CF_3$ yields, is observed already with small Ga additions, *i.e.* in Al/Ga-100-F with Al/Ga ratio of 100/1. It should be noted that general catalytic behaviour of the two Al-rich materials is very similar to that exhibited by fluorinated commercial γ-Al_2O_3 with considerably higher fluorine content used as a reference in a previous comparative study.[19] On the other side, further increase of Ga content strongly reduces catalytic activity w.r.t. CCl_2FCClF_2 isomerisation, as observed for the mixed Al/Ga-2-F. In line with this trend, fluorinated γ-Ga_2O_3, Ga#04-F, was catalytically completely inactive over the whole temperature range tested. In analogy with similar γ-Al_2O_3 systems, this could be ascribed to the low extent of fluorination, *i.e.* 3.6 wt.% of F (Table 1), that may be below the levels required to form sufficiently active surface sites. Namely, as found for fluorinated γ-Al_2O_3, approximately 10 atom% of anions must be replaced by F to achieve catalytic activity in dismutation of $CHClF_2$.[17] However, this reason can be ruled out since a low catalytic activity was observed also for the fluorinated mixed oxide with considerably higher F content, *i.e.* Al/Ga-2-F with 16.9 wt.% of F. This strongly suggests that, in contrast to the Al-sites, the Ga-related Lewis acid sites are not strong enough to catalyse the isomerisation of CCl_2FCClF_2. Furthermore, these findings also indicate that with increasing Ga levels the catalytic functionality of strong Al-related sites drops considerably. Higher levels of Ga do not simply lower the concentration of strong Al-related sites, but also obstruct their formation by preferential formation of Ga-sites, as suggested on the basis of PAS-py measurements mentioned above (see Section 3.3).

Catalytic tests also show that all active materials examined, Al#04-F, Al/Ga-100-F and Al/Ga-2-F, need a clear activation period in a stream of CCl_2FCClF_2 before they reach full catalytic activity. For the AlF_3-based catalysts, activation is associated with the removal of surface species that block Lewis acid sites. These species mostly originate from H_2O adsorption that besides blocking the Lewis acid sites leads to some hydrolysis and generates Brønsted acidity.[36,39] Activation of AlF_3-based catalysts, most frequently performed in situ by diverse fluorocarbons, can therefore be regarded as a re-fluorination process in which surface OH species are replaced by F. For the current fluorinated γ-Al_2O_3, sample Al#04-F, onset of catalytic activity is observed already at 573 K, while for the activation of both fluorinated mixed oxides, Al/Ga-100-F and Al/Ga-2-F, temperature of 623 K is required. Observed behaviour during activation correlates very well with much higher Brønsted acidity of the fluorinated mixed oxides in comparison with the single ones, as evidenced by PAS-py investigations (Fig. 5b).

Observed differences in catalytic performance of fluorinated Al- and Ga-rich mixed oxides do however not correlate with PAS-py observations. As noted above, PAS-py spectra of fluorinated single and mixed oxides, Figs. 5b and 6b, indicate the presence of Lewis acid sites that appear to be stronger in fluorinated mixed oxides. For the Al-rich mixed oxides these sites were associated with cus-

Table 3. Reaction of CCl_2FCClF_2 in contact with fluorinated single and representative mixed oxides under steady flow conditions; contact time 1 s, GC analyses done after 1 h equilibration at the temperature specified.

Sample	Temp.[a],K	Product distribution, relat. yield, %				
		$CClF_2CF_3$	CCl_2FCF_3 + $CClF_2CClF_2$[b]	CCl_2FCClF_2	CCl_3CF_3	CCl_3CClF_2
Ga#04-F	573*	0	0	100	0	0
	593*	0	0	100	0	0
	623*	0	0	100	0	0
Al/Ga-2-F	573*	0	0.5	99.5	0	0
	593*	0	1.5	98.2	0	0.4
	623*	0	7.2	84.0	3.3	5.5
	593	0	5.4	88.7	2.3	3.5
	573	0	3.5	94.8	0.4	1.4
	523	0	0.4	99.4	0	0.3
Al/Ga-100-F	573*	0	0	99.7	0	0.3
	593*	0	0.1	99.0	0	0.9
	623*	0.2	19.9	12.5	54.8	12.7
	593	0.3	19.5	3.4	70.6	6.2
	573	0.1	18.4	3.3	71.7	6.4
	523	0	18.4	18.6	55.5	7.5
Al#04-F	523*	0	0	100	0	0
	573*	0.3	22.4	2.9	71.3	3.1
	593*	0.3	19.7	3.2	71.4	5.3
	623*	0.6	24.0	3.9	67.1	4.3
	593	0.3	17.6	3.2	70.8	8.2
	573	0.2	16.5	2.8	73.6	6.8
	523	0	13.2	19.1	57.0	10.7

[a] Steps in the initial (activation) stage are marked with *.
[b] The two isomers were not separated by GC. Previous studies showed that the asymmetric isomer, CCl_2FCF_3, largely prevails.[10]

Al^{3+} ions, which are replaced by cus-Ga^{3+} ions in Ga-rich materials. Lower catalytic activity of the latter would therefore suggest that catalytic isomerisation of CCl_2FCClF_2 is taking place only on cus-Al^{3+} sites and not on cus-Ga^{3+} sites. The corresponding redshifts in PAS-py spectra are however very low, 1–2 cm^{-1} for the band at 1626 cm^{-1} (Fig. 6b), that does not allow an unequivocal assignment of these bands to specific cationic sites. In addition, recent XPS and *ab initio* investigations of AlF_3 materials stressed that Lewis acidity and catalytic activity can depend decisively on local geometric structure and stoichiometry, and not just on local coordination.[36] Furthermore, accessibility of active sites for both probe molecules, pyridine and CCl_2FCClF_2, may be different.

4. Conclusions

Single γ-Al_2O_3 and γ-Ga_2O_3, and mixed γ-Al_2O_3/γ-Ga_2O_3, used as precursors within this study, exhibit very low crystallinity and have high surface areas. Bulk structure of the mixed oxides is consistent with the formation of γ-Al_2O_3/γ-Ga_2O_3 solid solutions. Comparative spectroscopic investigations of acidity, performed by means of pyridine adsorption, show that Lewis acidity of mixed γ-Al_2O_3/γ-Ga_2O_3 is higher than that of both single oxides. Such synergetic effects on acidity of mixed γ-Al_2O_3/γ-Ga_2O_3 are well-documented. Our findings do however give new evidence for the formation of additional strong Lewis acid sites in mixed oxides with higher Ga contents. Lewis acidity of mixed γ-Al_2O_3/γ-Ga_2O_3 is therefore associated with the presence of surface cus-Ga^{3+} ions, mainly due to their strong preference to occupy tetrahedral positions. Namely, coordinatively unsaturated (cus) cations in tetrahedral positions are commonly related with the strongest Lewis acid sites found on these types of oxides.[42] Increase in the number of acid sites and formation of additional strong Lewis acid sites are both an indication that heterogeneity of mixed γ-Al_2O_3/γ-Ga_2O_3 surfaces is considerably higher than that of single oxides and is increasing with increasing Ga content. On the other side, XPS shows that surfaces of mixed oxides are enriched with Al, very likely through some reconstruction processes. All these observations clearly indicate that both composition and structure of surfaces in real mixed oxides may deviate considerably from those expected for an ideal solid solution.

Treatment of single and mixed oxides with CHF_3 at 623 K results in partial fluorination with concomitant reduction of surface areas. XPS confirms that under reductive conditions encountered during fluorination with CHF_3 Ga^{3+} is not reduced to lower oxidation states. Bulk struc-

ture of the oxide precursors is not affected by fluorination what indicates that fluoride phases initially formed are highly dispersed and amorphous. Appearance of distinctive $Al(F,OH)_3 \cdot nH_2O$ phases is correlated with slow post-crystallisation processes promoted by water adsorption. Preferential formation of Al–F based phases is additionally substantiated by XPS results which clearly showed that in fluorinated γ-Al_2O_3/γ-Ga_2O_3 F binds mainly to Al-atoms while Ga-atoms remain prevalently in O environments. XPS in addition showed that surfaces of fluorinated mixed oxides were enriched with Ga what is interpreted as formation of Al–F phases in the subsurface region what leads to the enrichment of Ga–O phases on the surface. These findings give strong evidence that fluorination of γ-Al_2O_3/γ-Ga_2O_3 surfaces is proceeding rather selectively what may lead to the formation of segregated (Al–F)-rich and (Ga–O)-rich regions.

As expected, partial fluorination of mixed γ-Al_2O_3/γ-Ga_2O_3 with CHF_3 increased the strength of Lewis acid sites due to the partial replacement of O/OH with F. Fluorination also reduced the heterogeneity of these acid sites probably due to some structural ordering. Similarly to the situation encountered with mixed oxides, number of acidic sites in fluorinated mixed oxides was higher than in fluorinated single oxides. Overall increase of Lewis acidity in fluorinated γ-Al_2O_3/γ-Ga_2O_3 observed by adsorption of pyridine was however not substantiated by catalytic activity w.r.t. isomerisation of CCl_2FCClF_2. Isomerisation activity was observed only for fluorinated oxides with lowest Ga contents. It was concluded that isomerisation is taking place only on cus-Al^{3+} sites that are stronger Lewis acids than cus-Ga^{3+} sites. Isomerisation of CCl_2FCClF_2 can therefore be used as a sensitive test to differentiate between these sites and can in this respect complement pyridine adsorption that appears to be not selective enough to discriminate between various cationic acid sites present on the surfaces of fluorinated γ-Al_2O_3/γ-Ga_2O_3.

Fluorination of γ-Al_2O_3/γ-Ga_2O_3 with CHF_3 at intermediate temperatures is demonstrated to be a versatile approach for the preparation of solid materials with some specific characteristics. On one side, partial fluorination of oxide precursors yields materials with surface areas above 100 $m^2\ g^{-1}$. On the other side, acidity is affected by both fluorination and preferential replacement of the most acidic cus-Al^{3+} ions with the less acidic cus-Ga^{3+} ions. All these aspect are important in the preparation of acidic materials with tailored characteristics for possible catalytic applications.

5. Acknowledgement

AV was funded by the Slovenian Research Agency (ARRS) through the young researcher programme (Contract No. 1000-08-310004). Authors are grateful to Asst. Prof. Srečo D. Škapin for XRD measurements.

6. References

1. C. O. Areán, A. L. Bellan, M. P. Mentruit, M. R. Delgado, G. T. Palomino, *Micropor. Mesopor. Mat.*, **2000**, *40*, 35–42.
2. A. Vimont, J. C. Lavalley, A. Sahibed-Dine, C. O. Areán, M. Rodríguez Delgado, M. Daturi, *J. Phys. Chem. B*, **2005**, *109*, 9656–9664.
3. K.-I. Shimizu, M. Takamatsu, K. Nishi, H. Yoshida, A. Satsuma, T. Tanaka, S. Yoshida, T. Hattori, *J. Phys. Chem. B*, **1999**, *103*, 1542–1549.
4. T. Nakatani, T. Watanabe, M. Takahashi, Y. Miyahara, H. Deguchi, S. Iwamoto, H. Kanai, M. Inoue, *J. Phys. Chem. A*, **2009**, *113*, 7021–7029.
5. M. Takahashi, N. Inoue, T. Takeguchi, S. Iwamoto, M. Inoue, *J. Am. Ceram. Soc.*, **2006**, *89*, 2158–2166.
6. M. Haneda, Y. Kintaichi, T. Mizushima, N. Kakuta, H. Hamada, *Appl. Catal. B: Environmental*, **2001**, *31*, 81–92.
7. M. Chen, J. Xu, F.-Z. Su, Y.-M. Liu, Y. Cao, H.-Y. He, K.-N. Fan, *J. Catal.*, **2008**, *256,* 293–300.
8. T. Olorunyolemi, R. Kydd, *J. Catal.*, **1996**, *158*, 583–586.
9. E. Kemnitz, J. M. Winfield, in: T. Nakajima, B. Žemva, A. Tressaud (Eds.), Advanced Inorganic Fluorides: Synthesis, Characterization and Applications, Elsevier Science S. A, Amsterdam, **2000**, chapter 12.
10. H. Bozorgzadeh, E. Kemnitz, M. Nickkho-Amiry, T. Skapin, J. M. Winfield, *J. Fluorine Chem.*, **2001**, *110*, 181–189.
11. T. Skapin, E. Kemnitz, *Catal. Lett.*, **1996**, 40, 241–247.
12. T. Skapin, *J. Mater. Chem.*, **1995**, *5*, 1215–1222.
13. H. Bozorgzadeh, E. Kemnitz, M. Nickkho-Amiry, T. Skapin, J. M. Winfield, *J. Fluorine Chem.*, **2001**, *107,* 45–52.
14. C. H. Barclay, H. Bozorgzadeh, E. Kemnitz, M. Nickkho-Amiry, D. E. M. Ross, T. Skapin, J. Thomson, G. Webb, J. M. Winfield, *J. Chem. Soc. Dalton Trans.* **2002**, 40–47.
15. W. Zhang, M. Sun, R. Prins, *J. Phys. Chem. B*, 2002, *106*, 11805–11809.
16. A. Hess, E. Kemnitz, *J. Catal.*, **1994**, *149*, 449–457.
17. O. Boese, W. E. S. Unger, E. Kemnitz, S. L. M. Schroeder, *Phys. Chem. Chem. Phys.*, **2002**, *4*, 2824–2832.
18. G. B. McVicker, C. J. Kim, J. J. Eggert, *J. Catal.*, **1983**, *80*, 315–327.
19. T. Skapin, Z. Mazej, A. Makarowicz, A. Jesih, M. Nickkho-Amiry, S. L. M. Schroeder, N. Weiher, B. Žemva, J. M. Winfield, *J. Fluorine Chem.*, **2011**, *132*, 703–712.
20. T. Olorunyolemi, R. A. Kydd, *Catal. Lett.*, **1999**, *63*, 173–178.
21. Z. M. El-Bahy, R. Ohnishi, M. Ichikawa, *Catal. Today*, **2004**, *90*, 283–290.
22. Z. M. El-Bahy, R. Ohnishi, M. Ichikawa, *Appl. Catal., B*, **2003**, *40*, 81–91.
23. V. G. Hill, R. Roy, E. F. Osborn, *J. Am. Ceram. Soc.*, **1952**, *35*, 135–142.
24. V. S. Escribano, J. M. G. Amores, E. F. Lopez, M. Panizza, C. Resini, G. Busca, *J. Mater. Sci.*, **2005**, *40*, 2013–2021.
25. R. Roy, V. G. Hill, E. F. Osborn, *J. Am. Chem. Soc.*, **1952**, *74*, 719–722.
26. M. Ponikvar, B. Sedej, B. Pihlar, B. Žemva, *Anal. Chim. Acta*, **2000**, 418, 113–118; J. F. Liebman, M. Ponikvar, *Struct.*

Chem., **2005**, *16*, 521–528.
27. A. Vakulka, G. Tavčar, T. Skapin, *J. Fluorine Chem.*, **2012**, *142*, 52–59.
28. J. F. Moulder, W. F. Stickle, P. E. Sobol, K. D. Bomben, Handbook of X-Ray Photoelectron Spectroscopy, Physical Electronics Inc., Eden Prairie, Minnesota, USA, **1995**.
29. H. Bozorgzadeh, E. Kemnitz, M. Nickkho-Amiry, T. Skapin, J. M. Winfield, *J. Fluorine Chem.*, **2003**, *121*, 83–92.
30. J. C. Lavalley, M. Daturi, V. Montouillout, G. Clet, C. O. Areán, M. Rodríguez Delgado, A. Sahibed-dine, *Phys. Chem. Chem. Phys.*, **2003**, *5*, 1301–1305.
31. C. O. Areán, M. R. Delgado, V. Montouillout, D. Massiot, *Z. Anorg. Allg. Chem.*, **2005**, *631*, 2121–2126.
32. JCPDS PDF-files: 41-0381, 18-0024 and 4-0196.
33. R. König, G. Scholz, R. Bertram, E. Kemnitz, *J. Fluorine Chem.*, **2008**, *129*, 598–606.
34. E. K. L. Y. Hajime, J. L. Delattre, A. M. Stacy, *Chem. Mater.*, **2007**, *19*, 894–902.
35. T. Skapin, G. Tavčar, A. Benčan, Z. Mazej, *J. Fluorine Chem.*, **2009**, *130*, 1086–1092.
36. A. Makarowicz, C. L. Bailey, N. Weiher, E. Kemnitz, S. L. M. Schroeder, S. Mukhopadhyay, A. Wander, B. G. Searle, N. M. Harrison, *Phys. Chem. Chem. Phys.*, **2009**, *11*, 5664–5673.
37. C. L. Bailey, S. Mukhopadhyay, A. Wander, B. G. Searle, N. M. Harrison, *J. Phys. Chem. C*, **2009**, *113*, 4976–4983.
38. L. Francke, E. Durand, A. Demourgues, A. Vimont, M. Daturi, A. Tressaud, *J. Mater. Chem.*, **2003**, *13*, 2330–2340.
39. T. Krahl, A. Vimont, G. Eltanany, M. Daturi, E. Kemnitz, *J. Phys. Chem. C*, **2007**, *111*, 18317–18325.
40. A. Serykh, M. D. Amiridis, *Surf. Sci.*, **2009**, *603*, 2037–2041.
41. J. Krishna Murthya, U. Groß, S. Rüdiger, E. Ünveren, E. Kemnitz, *J. Fluorine Chem.*, **2004,** *125*, 937–949.
42. C. Morterra, G. Magnacca, *Catal. Today*, **1996**, *27*, 497–532.
43. J. M. Winfield, *J. Fluorine Chem.*, **2009**, *130*, 1069–1079.
44. Yu. N. Pushkar, A. Sinitsky, O. O. Parenago, A. N. Kharlanov, E. V. Lunina, *Appl. Surf. Sci.*, **2000**, *167*, 69–78.
45. A. L. Petre, A. Auroux, P. Gélin, M. Caldararu, N. I. Ionescu, *Thermochim. Acta*, **2001**, *379,* 177–185.
46. G. Busca, *Phys. Chem. Chem. Phys.*, **1999**, *1*, 723–736.
47. K. Sohlberg, S. J. Pennycook, S. T. Pantelides, *J. Am. Chem. Soc.*, **1999**, 121, 10999–11001; K. Sohlberg, S. T. Pantelides, S. J. Pennycook, *J. Am. Chem. Soc.*, **2001**, *123*, 26–29.
48. D. Dambournet, H. Leclerc, A. Vimont, J.-C. Lavalley, M. Nickkho-Amiry, M. Daturi, J. M. Winfield, *Phys. Chem. Chem. Phys.*, **2009**, *11*, 1369–1379.
49. A. Vimont, J.-C. Lavalley, L. Francke, A. Demourgues, A. Tressaud, M. Daturi, *J. Phys. Chem. B*, **2004**, *108*, 3246–3255.
50. P. Michorczyk, E. Sikora, J. Ogonowski, *React. Kinet. Catal. Lett.*, **2008**, *94(2),* 243–252.
51. J. Krishna Murthy, U. Groß, S. Rüdiger, V. Venkat Rao, V. Vijaya Kumar, A. Wander, C. L. Bailey, N. M. Harrison, E. Kemnitz, *J. Phys. Chem. B*, **2006**, *110*, 8314–8319.
52. M. Nickkho-Amiry, J. M. Winfield, *J. Fluorine Chem.*, **2007**, *128*, 344–352.

Povzetek

Interakcije CHF_3 z γ-Al_2O_3, γ-Ga_2O_3 ter mešanimi γ-Al_2O_3/γ-Ga_2O_3 kserogeli pri prehodnih temperaturah vodijo do delnega fluoriranja. Fluorirani oksidi ostajajo amorfni in ohranijo znaten del začetne specifične površine; površine fluoriranih materialov na osnovi Al tako v vseh primerih presegajo 100 m^2 g^{-1}. Na Lewisovo kislost mešanih oksidov, tako pred kot tudi po fluoriranju, močno vpliva prisotnost površinskih Ga^{3+} ionov, predvsem zaradi preferenčne zamenjave močno kislih Al^{3+} ionov na tetraedrskih mestih. Zamenjava ionov vodi k nastanku manj kislih centrov, kar je bilo potrjeno z modelno katalitsko reakcijo, izomerizacijo CCl_2FCClF_2. XPS preiskave kažejo, da fluoriranje mešanih oksidov vodi do znatne rekonstrukcije površin ter do preferenčne tvorbe Al–F faz, medtem ko Ga ostaja predvsem v O okoljih. Nadaljnji segregacijski procesi, kot je npr. počasna kristalizacija $Al(F,OH)_3 \cdot nH_2O$ faz, najverjetneje potekajo zaradi adsorpcije vode.